DETAILS OF ANALYSIS OF AIRPLANE STRUCTURE ACOUSTIC LOADING IN FLIGHT TESTING

E.V.Arnautov
Flight Research Institute,USSR

Abstract

Current urgency of flight research into airplane structural component acoustic loading is noted. Outlines of the experimental data aquisition and reduction systems are described. Features of current commonly used autoregression method applications in spectral analysis, rejection and diagnostics are considered. Examples of dynamic strain flight tests of an inlet duct and pressure fluctuations on a passenger airplane flap are given.

Introduction

Many structural components of a modern airplane are subjected to high intensity aeroacoustic loads. Fluctuating pressures from various noise sources can produce vibrations of the components and high levels of the structure dynamic stresses. It results in high-cycle random fatigue failures (acoustic fatigue). Therefore, one of the important tasks of the airplane production is to study the behaviour and to develop methods for structural high acoustic load protection. Currently, the problem of acoustic fatigue became especially actual due to expansion of airplane operations, improvements in structural weight characteristics and higher requirements for airplane performance.

In most cases, failures due to acoustic load are detected before serious decrease in airplane strength occurs. It is often necessary, however, to undertake a large amount of repair and significantly increase requirements for routine inspections.

The highest dynamic response to acoustic load is typical for the external skin panels and substructure (stringers, ribs, frames, spars, clips, etc.). The problem of acoustic fatigue emerges for certain elements at the load level of I30 dB. The levels which exceed I50 dB are generally dangerous for typical thin-walled structural strength. At the same time, maximum noise levels can be higher than I70 dB.[1]

The predominant contribution to vibration power is usually made by a fundamental mode. For a number of structures, however, this rule does not work; for example, for cylindrical shells where many mode shapes of vibration are possible. This complicates the structure response study (localizations of zones of maximum stresses, individual mode contribution evaluation, choice of the structure modification).

Ordinarily, semi-empirical analysis and follow-on experiment are used to determine fatigue life under dynamic loading. However, under acoustic load the first step in evaluation of service life-time for many structural elements is flight testing. This is primarily explained by the fact that acoustic load characteristics for many airplane areas are known with low accuracy. In addition, the service lifetime for certain elements is not determined because of their "minor importance".

Analysis of acoustic loading is a complex task; to solve it, various factors should be accounted for. Inspite of the traditional methods used in flight tests, they are to be continuously developed. This is caused by new problems permanently arising in structural dynamics, improvements of data acquisition and reduction systems.

On-board instrumentation and ground data reduction systems

The main parameter for studying acoustic loading in flight are dynamic strains in the structure. Pressure fluctuations, static stresses and other low-frequency response parameters including airplane and flight parameters are also may be measured.

The dynamic processes under consideration have a wide frequency range (up to 5000 Hz), stochasticity, nonstationary character for some flight conditions, a large number of factors affecting the level and spectral composition of the processes.

There are two measurement approaches using strain gages in fatigue studies:

- the gages are positioned in the fatigue crack areas to measure maximum strains;
- the gages are positioned throughout the structure to determine strains in "regular" zones and to possibly estimate the mode shapes of vibration.

Since fatigue cracks usually emerge at places of high stress concentrations or their gradients, for example, in joints, the probability of maximum strain detection is negligible. In this case large strain gages (with a grid length of 5 to 20 mm) can average strain along the grid length, and small ones (with a grid length of 0.5-I.5 mm) do not provide the required surface coverage. Hence, the first approach can give wrong or defective results. The second way provides more true description of the structure response and stable results. Therefore, in flight test it is more reasonable to use the second approach. The information obtained in this way may provide a sufficiently adequate structure response in later fatigue tests, if the gage layouts in the airplane and on the test panels are the same. When using the design methods for the lifetime determination based on flight data, additional information on stress concentrators will be needed.

Data aquisition is made by the instrumentation system aboard the airplane (Fig.I). The data are usually recorded by a low-frequency response pulse-code-modulation (PCM) system and a high -frequency response modulation (FM) system. These data streams are recorded on a mag-

netic tape aboard the airplane during flight. Low-frequency response parameters, such as static stresses, static pressures, temperatures, flight and airplane parameters are recorded on the PCM system. High frequency parameters, such as dynamic strains, pressure fluctuations and vibrational accelerations are recorded on the FM system. The various parameters are filtered by the PCM instrumentation system before digitization to prevent aliasing errors.

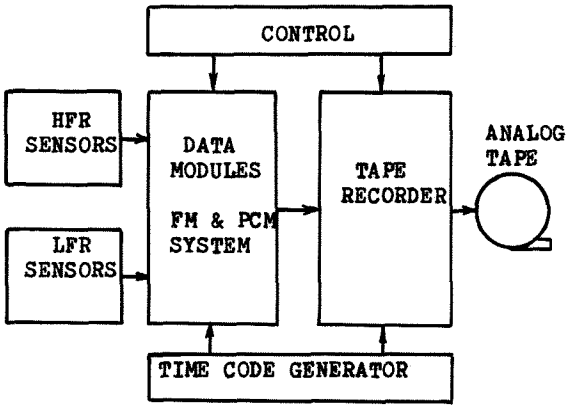

Figure I. Data aquisition system

Data from the instrumentation system recorded on the on-board magnetic tape, are processed by a ground system using analog and digital devices. For this, different configurations of the ground data processing system are used, but all of them consist of rather similar functional modules. A model structure of such a system is shown in Fig.2. The system is schematically shown as one-level from the computer-used point of view. Actually, it can be multilevel, where data from one computer to another is transferred with magnetic tapes, disks or with a communication link.

The data processing system performs the following operations:

- conversion of the FM and PCM data to a form suitable for the input into analog and digital reduction and visualization devices;
- input data monitoring;
- producing the rms time histories for dynamic processes;
- digital analysis of the data;
- screen data display, and also in a form of hard copies (lists and plots).

The data analysis software is typically organized into several major groups taken in series.

Initially, the data consolidation and editing program group is used for the information rejection and compression, correction of different errors, digital filtration, generation of the derived parameters, synchronization of the high and low frequency data.

The result of preliminary data processing is a digital data file which is further processed. The analysis programs contain the following:

- screening of the rms and peak level time histories;
- various kinds of spectral and cross spectral analysis,
- counting of peak occurrences,
- regression analysis,
- mode shape analysis,
- fatigue damage evaluation,
- generalization of the results from a variety of flights.

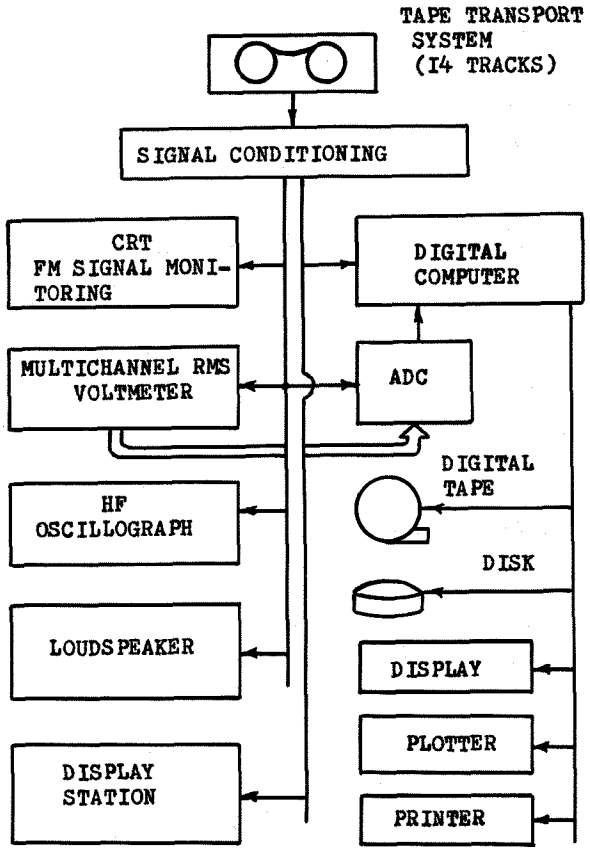

Figure 2. Data reduction system

Features of analysis using models

In current analysis of random processes including acoustic ones, an ever increasing part is assigned to modelling methods. It is due to the fact that a reasonably adequate model of a signal may be used not only for spectral analysis, but for some other purposes, such as signal prediction to control fatigue testing, data compression and correction, diagnostics, etc.

Power spectral density estimation

Consider a sequence

$$x_n = x(n\Delta t) ,$$

which is a sample from a random process with a constant frequency, f_s, that results in an equal time interval, Δt. Let the mean value $M[x_n] = 0$.

The linear estimate (LE) of the power spectral density (PSD) for a selected segment of the record (n=0,1,2, ..., N-1) can be found in terms

of the squared discrete Fourier transform[I]

$$G_I^*(f_m) = 2\Delta t\, N \left| \sum_{n=0}^{N-I} \gamma_n x_n e^{-i2\pi nm/N} \right|^2 \quad (I)$$

$$(m \leq N/2)$$

where γ_n is the weighting function in the time domain (data window). To improve the estimate (I) consistency, it may be smoothed with certain weights, H_m, in the frequency domain or by averaging over an ensemble.

The smoothed estimate (I) mean value is

$$M\left[G_I^*(f)\right] = \int_{-I/2\Delta t}^{I/2\Delta t} G(f-\lambda)\,\phi(\lambda)\,d\lambda \quad , \quad (2)$$

where G(f) is the PSD of x_n;

$$\phi(f) = \frac{\Delta t}{U} \sum_{m=-m_I}^{m_2} H_m \left| \sum_{n=0}^{N-I} \gamma_n e^{-2\pi(f-f_m)n\Delta t} \right|^2 ,$$

$$U = \sum_{n=0}^{N-I} \gamma_n^2 \quad ; \quad \sum_{m=-m_I}^{m_2} H_m = I$$

$\phi(f)$ function is called a spectral window. The linear estimate of the PSD can also be calculated with the correlation function, R_k^*

$$G_2^*(f_m) = 4\Delta t N \sum_{n=0}^{N-I} \lambda_k R_k^* \cos(\pi mk/N_I) \quad (3)$$

$$(m \leq N_I \leq N) \quad ,$$

$$R_k^* = \frac{I}{N} \sum_{n=0}^{N-I-k} x_n \gamma_n x_{n+k} \gamma_{n+k} \quad . \quad (4)$$

The mean value of estimate (3) takes the form of (2); its spectral window corresponds to a data window, γ_n, and a lag window, λ_n.

The bandwidth (resolution), ΔF, of the spectral estimates (I) and (3) is determined as half-power main peak width of $\phi(f)$ (Fig.3). For estimate (I) which is smoothed in the frequency domain, this width is of the order of $N_2/N\Delta t$, where $N_2=m_I+m_2+I$, and for estimate (3) with commonly applied Bartlett, Han, etc. windows, the width is of the order of $I/N_I\Delta t$. Since ΔF is predominant for statistical stability at about equal fall-off of $\phi(f)$ beyond the main peak, then, for the two estimates, the stability is provided by the equivalent number of the correlation points, $N_{eq.}=N_I=N/N_2$.

Nonlinear PSD estimate can be based upon a random process representation by the autoregressive model

$$x_n = \sum_{k=I}^{p} (-a_k x_{n-k}) + \delta_n \quad , \quad (5)$$

where δ_n is the noncorrelated prediction error.

The correspondent autoregressive estimate of the PSD is given by J.Makhoul[2] as

$$G_3^*(f) = \frac{Ep^*}{\left| I + \sum_{k=I}^{p} a_k e^{-2\pi ikf} \right|^2} \quad , \quad (6)$$

$$(\Delta t = 1) \quad .$$

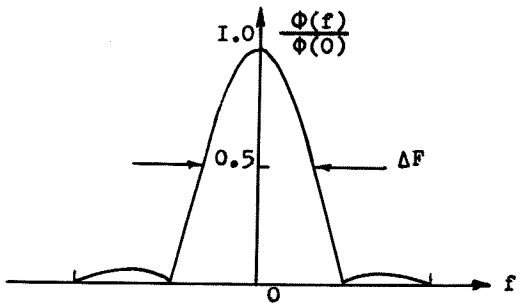

Figure 3. Determination of bandwidth for PS LE

Coefficients a_k can be computed from the correlation values, R_k^*, using Durbin[2] recursive procedure, and the error variance value is given by

$$E_p^* = R_o^* + \sum_{k=I}^{p} a_k R_k^* \quad (7)$$

To obtain p of a_k coefficients, p of the correlation function (R_k^*) values is used. As p increases to at least a certain value, E_p^* error decreases and the estimate of (6) approaches the actual PSD. However, because of the rounding-off errors, the convergence process, from a certain p number, may upset and E_p^* value will grow.

Correlation coefficients may be found directly or via inverse discrete Fourier transform from the PSD estimate

$$R_k^* = \frac{I}{N_3} \sum_{m=0}^{N_3-I} G_I(f_m) \cos\left(\frac{\pi mk}{N_3}\right) \quad , \quad (8)$$

where N_3 is the number of the PSD points within the frequency range (f_s, f_n) selected, with $0 \leq f_s < f_n \leq I/2\Delta t$. To eliminate R_k^* cycling, it is more correct to add zeroes to the original sequence x_n prior to calculating G_I^*.

The PSD AR does not have a fixed window of $\phi(f)$ and adaptively suppresses the components beyond the bandwidth. For time domain, it is equivalent to a prediction error minimization (δ_n), and for frequency domain, it equals the integral minimization

$$\int_o^{I/2\Delta t} (G/G_3^*)\, df \quad .$$

Up to now, methods for determination of the PSD AR statistical properties have not been developed. In this paper an attempt was made to assess these properties by analyzing various records of acoustic processes and dynamic stresses, obtained in flight test.

When comparing the PSD estimates, calculations were performed with formulas (I), (6), (7) and (8). The denominator in (6) had the form

$$\left| \sum_{k=0}^{N-I} a_k^* e^{-2\pi ikm/N_o} \right|^2$$

where a_k^* sequence was obtained by adding a certain number of zeroes to the sequence of $a_k = (I, a_I, \ldots, a_p)$, so that N_o was a power of 2. This method also yields a necessary interval in the frequency domain. In calculating estimate (I), constant weights, γ_n and H_m, were used. The averaging was performed over the frequency or over an ensemble, as well as with a combination of these methods.

The analysis of the results obtained shows the following:

- E_p^* error value most noticeably decreases with the coefficient p number increase from I to 30-50, that is due to the nature of the dynamic process correlation function;

- when attaining statistical proximity (in variance and bias) of the PSD AR and LE, the number of p was , on the average, by the order of magnitude less than that of the correlation point required to obtain LE with a given bandwidth, ΔF;

- any PSD, irrespective of the method, can be fairly well approximated with a model of AR, if nearly five model coefficients are to be taken for each significant PSD peak.

Obviously, minimum information fully determining the smoothed PSD LE is contained directly in its values, the latter being half the correlation point number. For the PSD AR, such information is contained in a_k coefficients. That is why, the second of the conclusions shows the possibility of compressing the information on acoustic process spectrum using the model.

Figures 4 and 5 show the properties of the PSD AR. The PSD estimates for a given example were determined for 40 adjacent segments of the dynamic pressure record. Initial parameters for a segment were f_s=4096 Hz, N=2048, p=79.

Figure 4 is a presentation of the PSD LE and AR mean values in the frequency range of 0 to 2048 Hz, with the PSD LE being smoothed within the band ΔF=8Hz (N_2=4). Figure 5 shows the mean values, as well as lower and upper envelopes for the whole set of the PSD LE and AR considered in the frequency range of I024-I536 Hz with the linear estimation bandwidth ΔF=4Hz.

It is seen that peak and mean values of the statistics considered are in close agreement with a certain preference for the AR estimates.

The given analysis showed that for a preliminary choice of the PSD AR coefficient numbers, an empirical formula may be used

$$p = \frac{f_s}{20\Delta F}$$

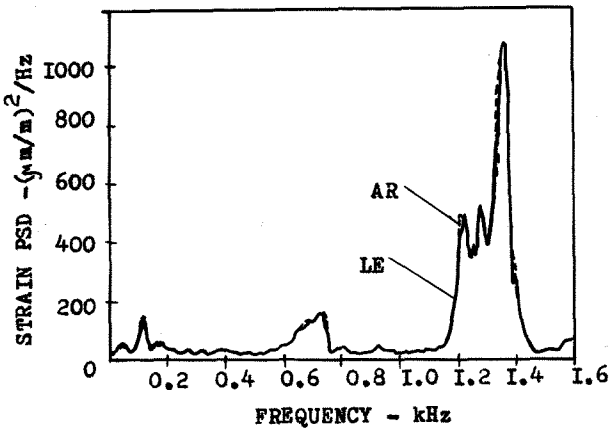

Figure 4. Comparison of linear and autoregressive PS estimates

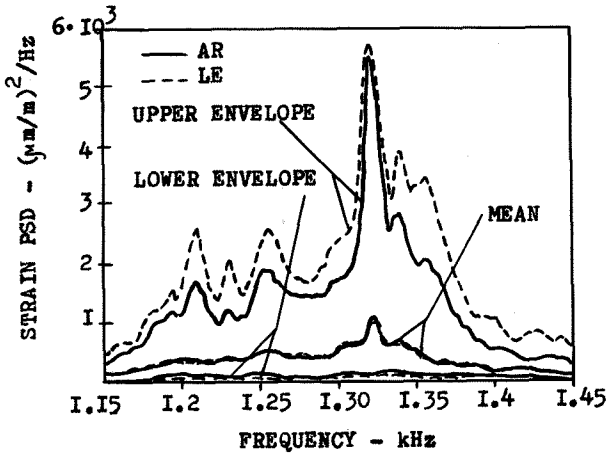

Figure 5. Comparison of upper and lower envelopes and mean values for PS LE and AR

In this case the relative rms error, δ, of the PSD AR will not be worse than that of the LE, for which $\delta \approx I/\sqrt{\Delta F \cdot T}$.

Rejection and diagnostics

Autoregressive model can be used to reject a real process. The following relationship is used as a criterion

$$|\varepsilon_n| = \left| x_n - \sum_{k=I}^{p} (-a_k x_{n-k}) \right| \leq \varepsilon_{max} .$$

To determine a threshold value δ_{max}, δ_n scatter is first found by processing a good signal over a sufficiently long record segment.

Similarly, diagnostics of the test structure condition can be carried out in long testing. In this case, if δ_n values are beyond the obtained δ_n scatter domain for a "healthy" object, the object under diagnosis is considered to have a defect.

Examples of flight tests

The examples given below confirm the conclusion that the nature of acoustic loading and structure response variations in flight is rather complicated, and such variations are unlikely predicted analytically.

Dynamic strains

Structure response is considered for flight test of Yak-42 inlet loading, having a turbofan engine. The main element under study was the sound-absorbing structure comprising a cylindrical frame-stiffened shell. The external streamlined surface of the shell was made of a perforated aluminium sheet and the internal one was made of glass fiber with honeycomb between them.

In flight test, the structure was instrumented with single-element strain gages to measure dynamic and static strains. The temperature was also monitored. The arrangement of the main strain gages for dynamic strains is given in Figure 6. The instrumentation frequency range was 20 to 5000 Hz.

In testing, typical operational conditions were flown along with special ones, such as

- vertical manoeuvres with n_y=I.5 at H= 3000 m and V_i=500 km/h
- left and right slipping at H=9000 m, V_i=500 km/h
- emergency descent from H=9000 m to H=3000 m.

Rms dynamic strain (σ_δ) variation with fan speed increase during ground run-ups (V=0) is given in Figure 7. The highest response is generally observed at 4I50 and 4700 r.p.m., that is less than maximum of 4950 r.p.m.Figure 8 illistrates σ_δ versus speed during take-off running and initial climb. In flight, the value of σ_δ was 2 to 3 times less than during take-off. The relationship in Figure 8 is due to acoustic load change with flight speed variations. This load is governed by the in-duct flow condition and fan noise (multiple pure tones) which depends on the tip Mach number.

The main spectrum part for the shell was within the frequency range up to I000 Hz and for the frames it was up to 2000 Hz (Figs.9-I0). The frames were the most heavily loaded structural elements. They had substantial broadening of the frequency range observed in flight as compared to take-off running conditions.

Static stresses were low and reached maximum values in flight.

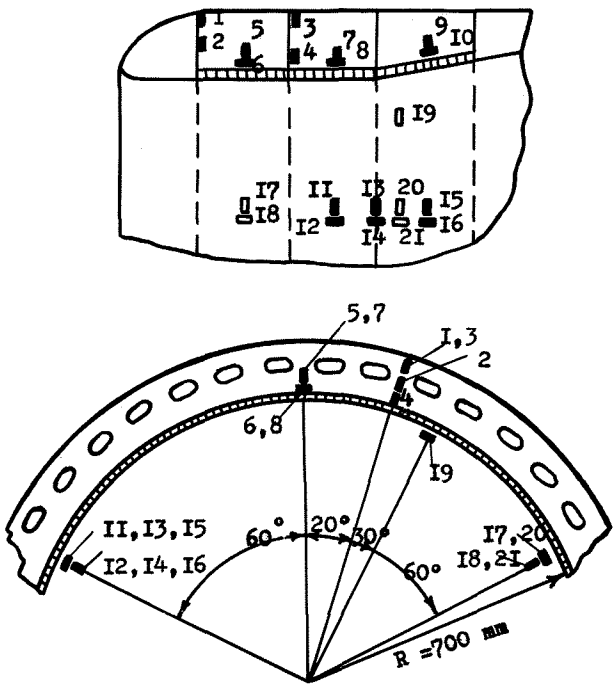

Figure 6. Fan duct inlet (Yak-42) dynamic strain gage locations

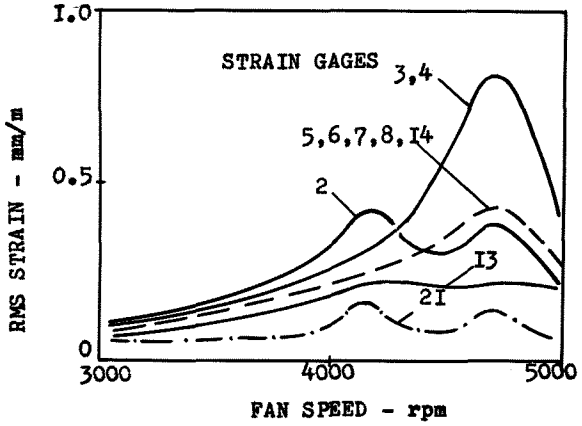

Figure 7. Strain vs fan speed in ground run

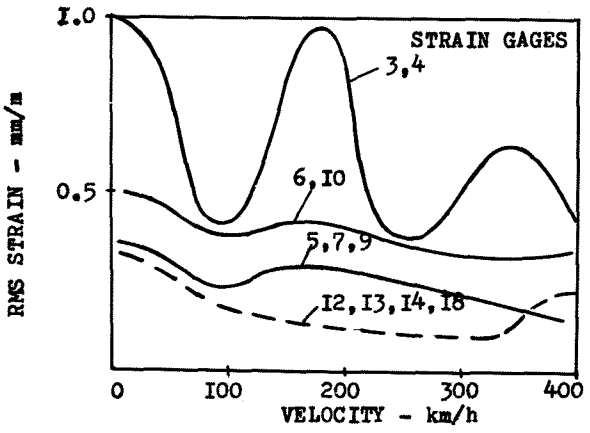

Figure 8. Variation of strain response with airplane velocity during take-off

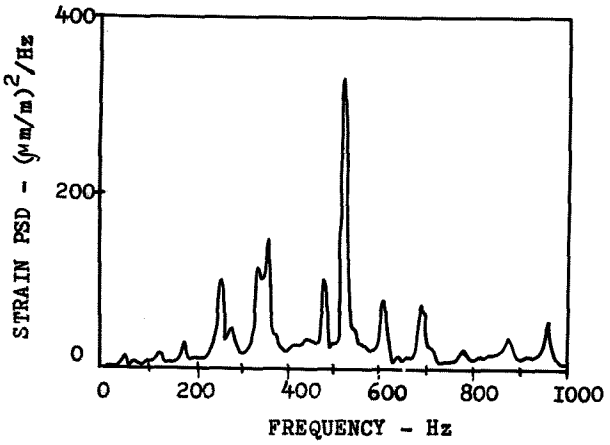

Figure 9. Strain power spectrum during take-off (4950 r.p.m.) - gage 7

Pressure fluctuations

As an example of pressure fluctuation study, some features of Il-86 flap acoustic loading in flight with a fully extended flap (δ_{fl} =40°) were considered. The fluctuating pressures were measured with piezoresistive transducers having an amplitude range P= ± 3000 Pa and a frequency range from 2 to 2500 Hz. A total of I0 transducers was installed (Fig.II).

Data analysis showed that the flap extention resulted in increase of the rms pressure fluctuation levels, σ_p, from 6 to I0 times as large as compared to the retracted position. For the upper surface, these levels increased in proportion to the dynamic pressure, q :

σ_p= 0.05 - 0.08 q .

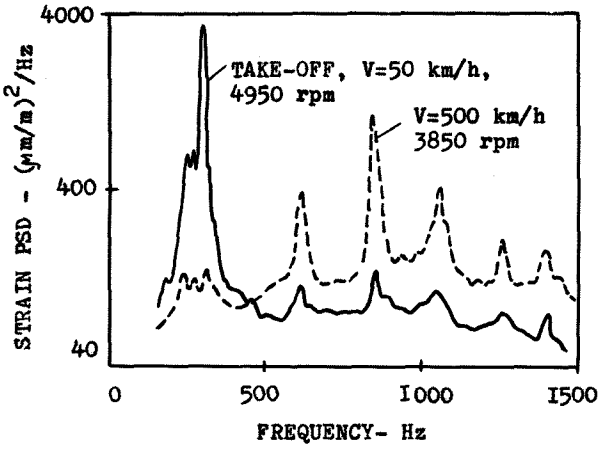

Figure I0. Strain power spectrum - - gage 3

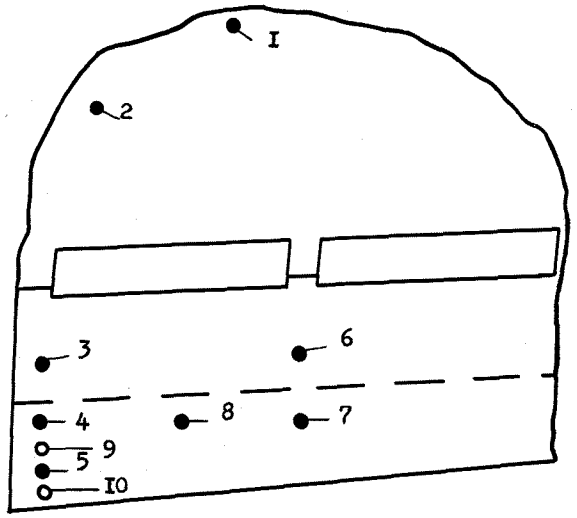

● UPPER SURFACE
○ LOWER SURFACE

Figure II. Il-86 flap fluctuating pressure transducer locations

On the lower surface σ_p values greatly depended upon the engine operating conditions growing fivefold at idle to rated power. In this case 50% fluctuation power was in the range of 40-300 Hz, and for the upper surface it was 2 to 40 Hz. However, the levels on the wing upstream the flaps were close to theoretical for a boundary layer (σ_p= 0.006 q),

and the spectrum was uniform (Fig.I2). Going into engine reverse during the airplane ground run resulted in proximity of fluctuation spectra on the upper and lower surfaces.

Coherence of fluctuations on the upper surface was significant (γ^2 =0.8) in the range of 6 to II Hz for points 3-5 and 6-IO.

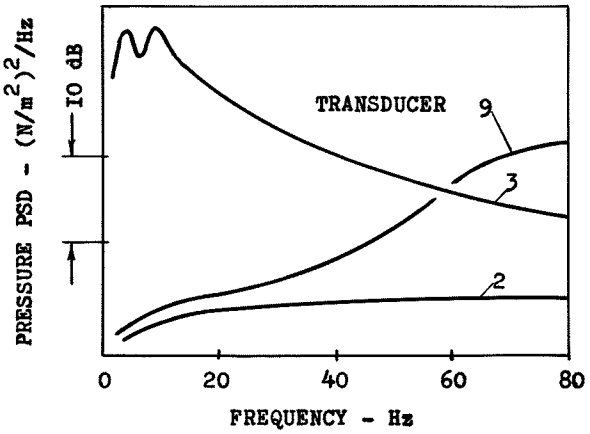

Figure I2. Fluctuating pressure power spectra

Conclusions

Flight research is a necessary phase of determination of the airplane structure acoustic fatigue. For some elements, the objective data can only be obtained in such research to evaluate the fatigue life and to perform necessary modifications to the structure.

Using the models of the structure dynamic loading for the estimation of power spectral density results in certain benefits as compared to traditional methods.

References

I. M.D.Klyatchko, E.V.Arnautov, "Flight strength testing. Dynamic loading: Handbook". Moscow, Machinostroenje, I984

2. J.Makhoul, "Linear prediction: a tutorial review", IEEE Transactions, I975, N4, p.20-44